Article:
Almeida, T.P., Fallon, K., Dugato, D.A. et al. (8 more authors) (2025) Advancing Lorentz Microscopy for Studying Magnetic Configurations in Next Generation Spintronic Devices and 3D Curved Magnets. Microscopy and Microanalysis, 31 (Supplement_1). ozaf048.1122. ISSN: 1431-9276

https://doi.org/10.1093/mam/ozaf048.1122

Advancing Lorentz Microscopy For Studying Magnetic Configurations in Next Generation Spintronic Devices And 3D Curved Magnets

Trevor P. Almeida[1]*, Kayla Fallon[1], Danian A. Dugato[2], Wesley B. F. Jalil[2], András Kovács[3], David Cooper[4], Flavio Garcia[2], Thomas Moore[5], Christopher H. Marrows[5], Rafal E. Dunin-Borkowski[3], Stephen McVitie[1]

[1]SUPA, School of Physics and Astronomy, University of Glasgow, Glasgow G12 8QQ, UK.
[2]Centro Brasileiro de Pesquisas Físicas (CBPF), Rua Dr Xavier Sigaud 150, Urca, 22290-180, Rio de Janeiro-RJ, Brazil.
[3]Ernst Ruska-Centre for Microscopy and Spectroscopy with Electrons (ER-C), 52425 Jülich, Germany.
[4]Univ Grenoble Alpes, CEA, LETI, Minatec campus F-38054, Grenoble, France.
[5]School of Physics and Astronomy, University of Leeds, Leeds LS2 9JT, United Kingdom
* Corresponding author: trevor.almeida@glasgow.ac.uk

To better understand the functional performance of modern spintronic devices, it is often necessary to investigate the underlying processes on the nanoscale. Lorentz transmission electron microscopy (TEM) techniques such as electron holography or differential phase contrast (DPC) imaging allows for the imaging of magnetic configurations in nanostructures with spatial resolution ≤ 1 nm. Adding the influence of external stimuli, e.g., biasing, heating, etc., through innovative *in-situ* TEM holders can further elucidate their dynamic magnetic behavior on the localized-scale operando conditions. In this context, several examples of the use of Lorentz TEM and *in-situ* experiments will be presented.

Equiatomic iron-rhodium (FeRh) has attracted much interest due to its magnetostructural transition from its antiferromagnetic (AF) to ferromagnetic (FM) phase and is considered desirable for potential application in a new generation of novel nanomagnetic or spintronic devices. Several scanning TEM techniques are performed to visualize the localized chemical, structural and magnetic properties of a series of cross-sectional and planar FeRh thin films [1-3].

Fig. 1a-c presents a cross-section of an Ir / Pd gradient-doped FeRh thin film (Fig. 1a), where energy dispersive x-ray (EDX) chemical maps (Fig. 1b) display the dopant profile of Pd (uniform) and Ir (gradient from top to bottom) [2]. The DPC images of Fig. 1c presents the AF / FM phase boundary (PB) motion with temperature, where no magnetic signal is evident in the AF Ir-rich side of FeRh thin film at 50°C and is separated from green FM region by an AF/FM PB. As temperature is increased, the green FM domain migrates upwards, inducing upward PB motion, until the FeRh film is fully FM at 200°C.

The DPC images of planar FeRh thin films in Fig.1d-f present information on the AF/FM domain evolution with heating and current pulse (CP) induced DW motion. Fig. 1d reveals the nucleation of vortex magnetic domains (labelled 'v') in a planar FeRh sample at 75°C and provides evidence of AF/FM phase co-existence [3]. The DPC image of Fig. 2e shows the planar FeRh sample in a FM state at 150°C with well-resolved DWs, which are then shown in Fig. 2f to be driven in an upwards direction by the application of 500μs CPs with a current density of ~ 2.2×10^9 A/m^2 (arrowed). Hence, Figure 1 has shown that PB motion in FeRh cross-sections can be controlled using Ir-gradient doping, the magnetostructural transition proceeds via nucleation of small vortex structures and application of CPs allows for current-driven DW motion in planar FeRh thin films.

Perpendicular shape anisotropy (PSA) and double magnetic tunnel junctions (DMTJs) offer practical solutions to downscale spin-transfer torque magnetic random-access memory (STT-MRAM) beyond 20 nm technology nodes. However, as these modern devices become smaller and three-dimensionally (3D) complex, our understanding of their magnetic behavior often relies on magnetoresistance measurements and micromagnetic modeling. Here, we present the stacking of

electron holograms to improve phase sensitivity and allows the imaging of the thermal stability of <20 nm PSA-STT-MRAM nano-pillars and subtle variations in DMTJs induced by annealing.

The high-angle annular dark-field (HAADF) scanning TEM (STEM) image (Fig. 2a) reveals the general morphology of a NiFe-based nanopillar, whilst the combined EDX / magnetic induction map (Fig. 2b) demonstrates the magnetization lies along the elongated axis of the NiFe section (~ 20 diameter, ~ 60 nm height), as indicated by the white arrow. Subsequent magnetic induction maps acquired during *in-situ* heating to 250°C demonstrate the nano-pillar to retain this direction of magnetization and confirms that the high-aspect-ratio NiFe section provides out-of-plane PSA that is resistant to thermal variations during operation [4].

The HAADF STEM image (Fig. 2c) and combined EDX / magnetic induction map (Fig. 2d) displays the morphology of a DMTJ (~ 60 nm height, ~ 35 nm largest diameter) and its multi-layered composition of Co (20 nm) / MgO (2 nm) / FeCoB (20 nm) / MgO (2 nm) / Co (20 nm). Fig. 2d shows that magnetization lies along the elongated axis of the DMTJ. Annealing to 400°C *in-situ* induces the magnetization to flow in a transverse direction across the central FeCoB layer and deviate away from the long axis in the top Co layer (Fig. 1e). This demonstrates that heating to 400°C chemically alters the multi-layered structure through diffusion and intermixing, degrading both the magnetic properties of individual layers and their exchange interaction across their interfaces [5].

Magnetic textures in self-supported nanostructures, such as vortex or skyrmion states, are promising for magnetic hyperthermia therapy and spintronics due to their low remanent state and topological protection. This work presents the use of colloidal lithography to fabricate curved nanocaps (Fig. 3a) [6] with unique magnetic properties. Single-layer permalloy ($Ni_{80}Fe_{20}$) nanocaps were systematically studied using micromagnetic simulations to create a phase diagram showing the ground magnetic state in relation to nanocap thickness and diameter, varying from onion to vortex states (Fig. 3b). Electron holography experimentally confirmed that nanocaps with diameter of 500 nm and thicknesses of 10 nm, 20 nm and 50 nm (Fig. 3c,d), all exhibited a vortex magnetic configuration as the ground state.

Multi-layered [Pt(1 nm)/Co(t)/Pt(1 nm)]×10 nanocaps with varying Co thickness (t) were simulated using micromagnetic modelling to show the ground state in relation to effective radial anisotropy constant (K_{radial}) and interfacial Dzyaloshinskii-Moriya interaction (iDMI), varying from vortex, planar ring, stripe, radial state and skyrmionics states (Fig. 3e). The K_{radial} resulting in skyrmionic states corresponded to 2 nm thick Co layers and was examined experimentally using electron holography. The nanocap curvature provides a tilt angle required for electron holography to be sensitive to the in-plane magnetic component, ϕ_m, of Néel-type skyrmions. The phase image (Fig. 3f) and magnetic induction map (Fig. 3g) confirms the presence of a single Néel-type skyrmion (labelled 'sk') and is consistent with that observed from Néel skyrmions in thin films [3,4]. Some nanocaps with 2 nm thick Co layers are observed to comprise two skyrmions, whilst nanocaps with 1.5 nm thick Co layers are consistent with stripe domain states. This works provides fundamental insight into the impact of geometric curvature on controlling ground states and iDMI, allowing effective engineering of vortex and skyrmionic configurations without the need to apply fields at room temperature.

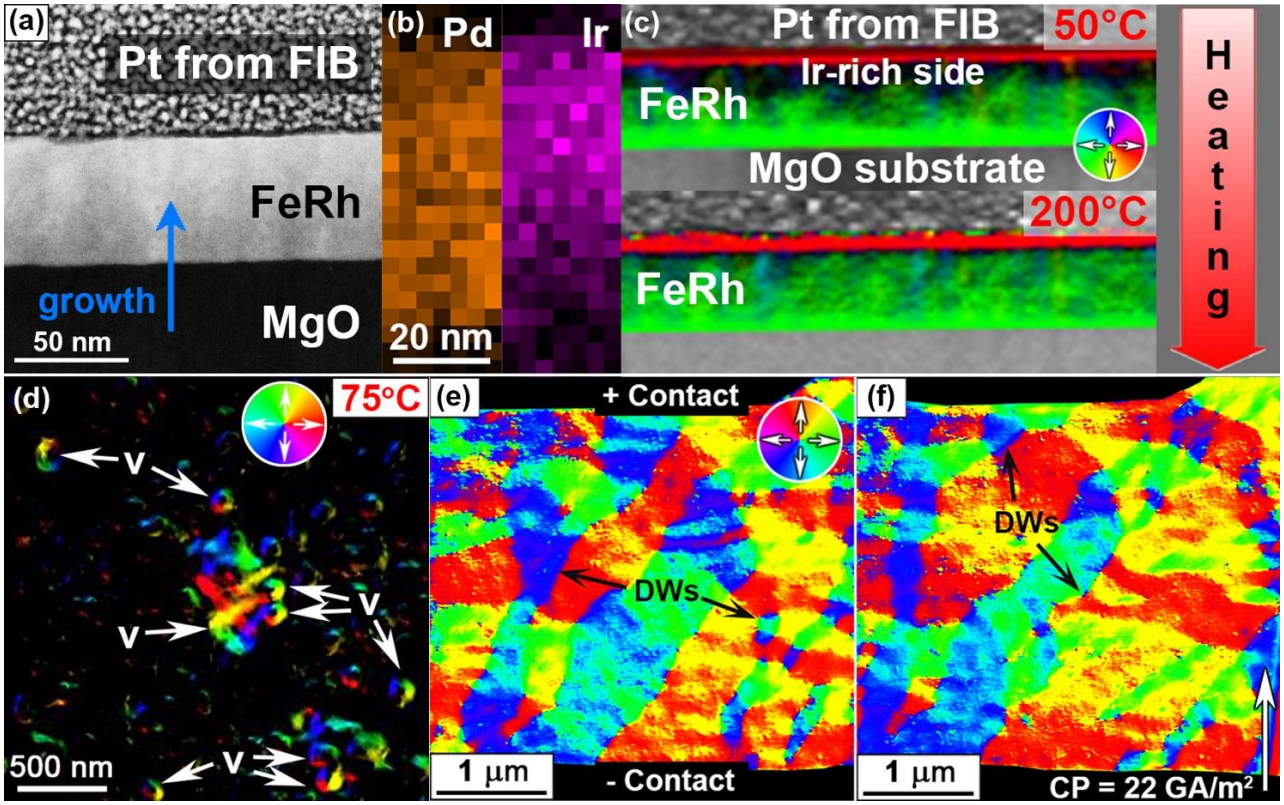

Fig. 1. (a) HAADF STEM image of an FeRh thin film; (b) EDX chemical maps showing the dopant distribution of Pd (orange, uniform) and Ir (pink gradient from top to bottom). (c) DPC imaging of the Ir/Pd gradient-doped FeRh film as a function of increasing temperature, displaying the upward PB motion to the Ir-rich side. (d) DPC imaging of a planar FeRh thin film showing (a) nucleation of vortex domains at 80ºC (denoted by 'v'); and (e,f) DWs in a planar FeRh thin film heated to (e) 150ºC; and (f) after application of 500μs CPs with a current density of ~ 2.2×10^{10} A/m^2 in the arrowed direction. The direction of magnetization in (c-f) is depicted in the color wheels (inset).

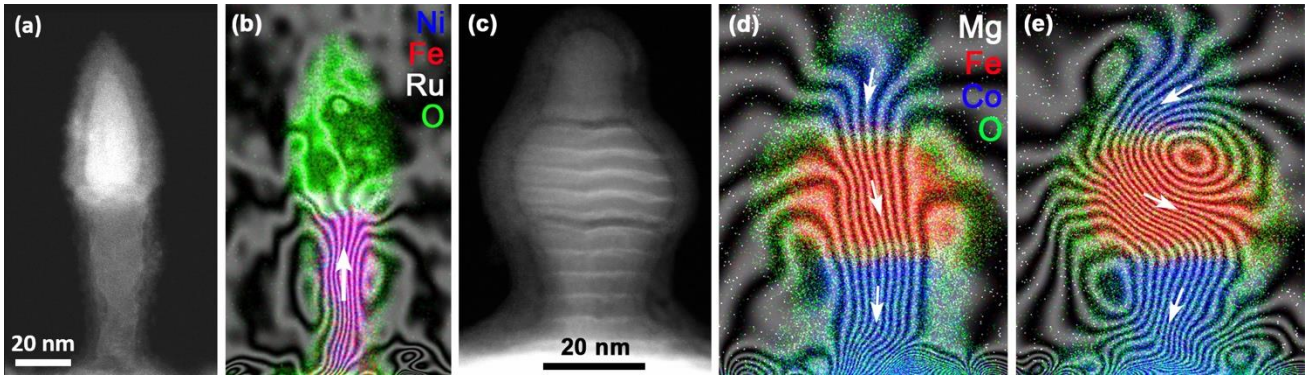

Fig. 2. (a) HAADF STEM image of a PSA nanopillar with a diameter of ~ 20nm; and (b) combined EDX / magnetic induction map showing the magnetization oriented along the long axis of the NiFe section. (c) HAADF STEM image of a multi-layered DMTJ nanopillar; and (d,e) combined EDX / magnetic induction maps (d) before; and after (e) *in-situ* heating annealing to 400C for 30 minutes.

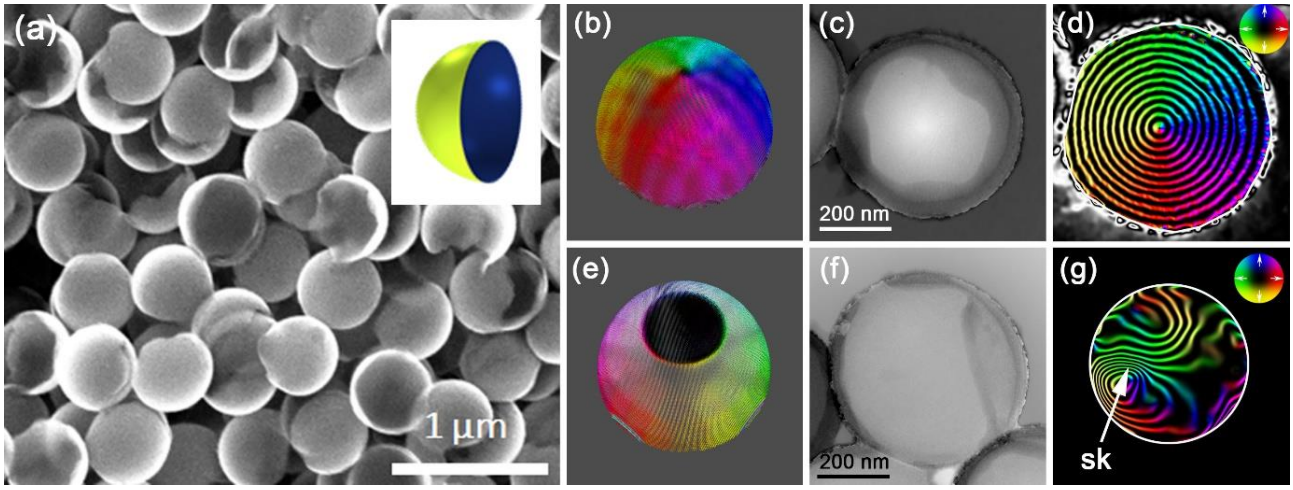

Fig. 3. (a) SEM image of nanocaps (d = 500 nm) produced by colloidal lithography and schematic of their idealized geometry (inset). (b) Micromagnetic simulation; (c) electron holography phase image and (d) associated reconstructed magnetic induction map of a permalloy nanocap showing its vortex configuration. (e) Micromagnetic simulation; (f) phase image and (g) associated reconstructed magnetic induction map of a multi-layered [Pt(1 nm)/Co(2 nm)/Pt(1nm)]×10 nanocap confirming the presence of a single Néel-type skyrmion (labelled 'sk'). The contour spacings are (d) 1.26 rad and (g) 0.157 rad, and the direction of magnetic induction is indicated by the color wheel (inset).

References:

[1] Almeida, T. P. *et al.* Scientific Reports (2017) **7**, 17835. https://doi.org/10.1038/s41598-017-18194-0

[2] Temple, R. C. *et al.* Applied Physics Letters (2021) **118**, 122403. https://doi.org/10.1063/5.0038950

[3] Almeida, T. P. *et al.* Physical Review Materials (2020) **4(3)**, 034410. https://doi.org/10.1103/PhysRevMaterials.4.034410

[4] Almeida, T. P. *et al.* Nano Letters (2022) **22**, 4000–4005. https://doi.org/10.1021/acs.nanolett.2c00597

[5] Almeida, T. P. *et al.* APL Materials (2022) **10**, 061104 https://doi.org/10.1063/5.0096761

[6] Jalil, W. B. F. *et al* Journal of Physics D: Applied Physics (2023) **56**, 385001. https://doi.org/10.1088/1361-6463/acdaa8